

## Time Series Analysis of Neurons and Visualization of Network Characteristics

Yoko Uwate<sup>†</sup>, Marie Engelene J. Obien<sup>‡</sup>, Urs Frey<sup>‡</sup> and Yoshifumi Nishio<sup>†</sup>

<sup>†</sup> Dept. of E. E. Eng., Tokushima University  
2-1 Minami-Josanjima Tokushima 770-8506 Japan  
Phone: +81-88-656-7662  
E-mail: {uwate, nishio}@ee.tokushima-u.ac.jp

<sup>‡</sup> MaxWell Biosystems  
Mattenstrasse 26, 4058 Basel, Switzerland  
Phone: +41-61-551-1070  
E-mail: {marie.obien, urs.frey}@mxwbio.com

### Abstract

In this study, we use nonlinear time-series analysis applied to neuronal data for visualizing specific characteristics of neuronal activity. We used extracellular spike recordings of a neuronal cell culture, observed at three different days in vitro. By applying three nonlinear time-series analysis, we confirmed that the neuronal culture has the highest activity during early network development and the neuronal activity settles down as the culture becomes mature.

### 1. Introduction

Understanding how brain circuits develop and operate is a major goal for many neuroscience projects. Burst patterns in neuronal networks may have an important role in information processing in the brain. Therefore, detecting and analyzing burst patterns are investigated in various fields [1]. Although it is important to study burst patterns in order to understand the correlation and communication processes of neurons, unveiling a structure of the whole neuronal network is also required.

Nonlinear time-series analysis is a useful tool for characterizing the dynamics behind the observed time-series data [2]. The neuronal data obtained from living neurons should be high-dimensional and of dynamic nature. In such a case, nonlinear time-series analysis can be used to characterize the neuronal data. Here, three techniques are applied: attractor reconstruction, recurrence plot and Lyapunov exponent.

In this study, we focus on time-series data generated from spike time data of neurons in culture. The spike times are detected using a high-density microelectrode array (HD-MEA) system [3] called MaxOne (MaxWell Biosystems, Basel, Switzerland). The system features 26,400 electrodes in total and a sampling rate of 20 kHz. We chose a recording time of 60 seconds. First, we detect the spikes per electrode and visualize the spike times in a raster plot. Next, we convert the spike time data to time-series data by calculating the spike rate of all electrodes per time bin. Finally, we apply nonlinear time-series analysis to the three time-series data from a neuronal culture measured at days in vitro (DIV) 15, 20 and 30,

respectively. By using computer simulations, we confirm that the characteristics of these neuronal networks change across different DIV.

### 2. Neuron data set

#### 2.1 Measurement platform

We used a CMOS-based high-density microelectrode array (HD-MEA) system called MaxOne (MaxWell Biosystems, Basel, Switzerland) composed of 26,400 platinum electrodes in a regular grid format with 17.5  $\mu\text{m}$  electrode center-to-center distance (3,265 electrodes/ $\text{mm}^2$ ). Up to 1,024 electrodes could be simultaneously recorded by routing the electrodes to low-noise read-out channels through a flexible switch-matrix approach [4]. On-chip circuitry was used to amplify (0-78 dB programmable gain), filter, and digitalize (10-bit, 20 kHz) the recorded signals. Online spike detection was performed by the MaxLab Live software (threshold:  $\times 5$  RMS noise).

#### 2.2 Cortical cell cultures

Primary cell cultures were prepared as described in Ref. [5], in accordance to Swiss Federal Laws on animal welfare. Briefly, cells from embryonic day 18 Wistar rat cortices were dissociated in 2 ml of trypsin with 0.25 % EDTA (Invitrogen, California, USA) with trituration.

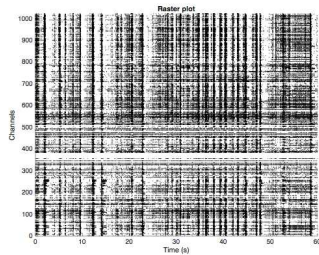
The electrode array surface was pre-coated with a thin layer of poly (ethyleneimine) (Sigma, Missouri, USA), 0.05 % by weight in borate buffer (Chemie Brunschwig, Basel, Switzerland) at 8.5 pH, followed by a 10 ml drop of 0.02 mg/ml laminin (Sigma) in Neurobasal medium (Invitrogen, California, USA) for cell adhesion. 20000-30000 cells in an 8-l drop were seeded over the array, and 1 ml of plating medium was added after 20 minutes. After 24 hours, the plating medium was changed to growth medium. Plating medium consisted of 850 ml of Neurobasal, supplemented with 10 % horse serum (HyClone, Utah, USA), 0.5 mM GlutaMAX (Invitrogen, California, USA) and 2 % B27 (Invitrogen, California, USA). Growth media consisted of 850 ml of DMEM - Dulbecco's Modified Eagle Medium (Invitrogen, California,

USA), supplemented with 10 % horse serum, 0.5 mM GlutaMAX and 1 mM sodium pyruvate (Invitrogen, California, USA). The cultures were maintained inside an incubator to control environmental conditions (37°C, 65 % humidity, 9 % O<sub>2</sub>, 5 % CO<sub>2</sub>) in 1 ml of growth medium (partially replaced twice per week).

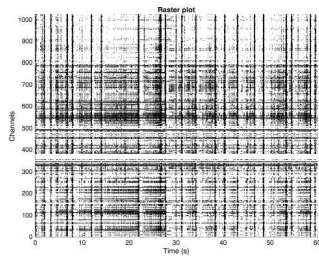
### 2.3 HD-MEA extracellular recordings

The MaxOne HD-MEA recording setup was placed in a recording incubator (65 % humidity) to ensure controlled environmental conditions (36°C and 5 % CO<sub>2</sub>). During experiments, the MaxOne chips were transferred to the recording incubator and covered with sterilized lids to minimize media evaporation. Cultures were recorded at DIV 15, 20, and 30.

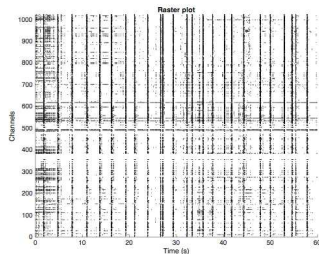
Figure 1 shows the raster plot obtained from the same neuronal culture across multiple days; DIV 15, 20 and 30, using 1,024 electrodes. Next, we calculate the spike rate at time bins, then time-series data is obtained as shown in Fig. 2.



(a) DIV 15.

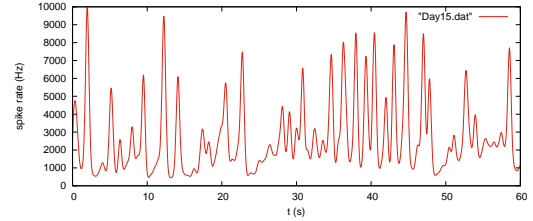


(b) DIV 20.

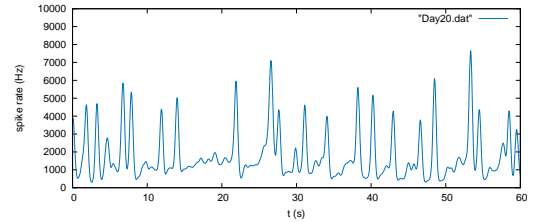


(c) DIV 30.

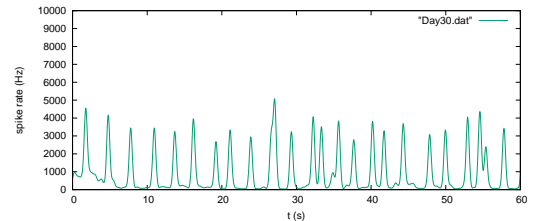
Figure 1: Raster plot of neurons from 1,024 electrodes.



(a) DIV 15.



(b) DIV 20.



(c) DIV 30.

Figure 2: Time series data of the neurons.

## 3. Simulation results using nonlinear time-series analysis

In this section, we explain three techniques of nonlinear time-series analysis and show the results.

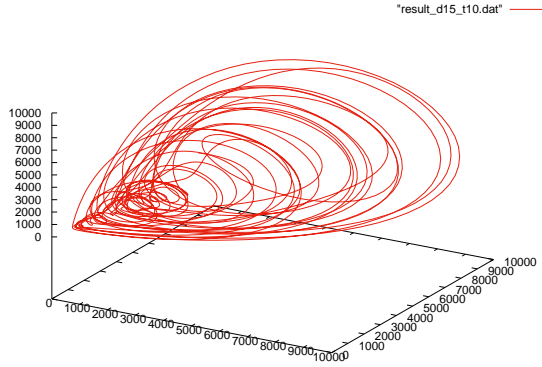
### 3.1 Attractor reconstruction

The attractor of dynamical systems can be reconstructed topologically in the embedding space from Takens' theorem [6]. The state vectors in the reconstructed  $m$ -dimensional embedding space are defined by

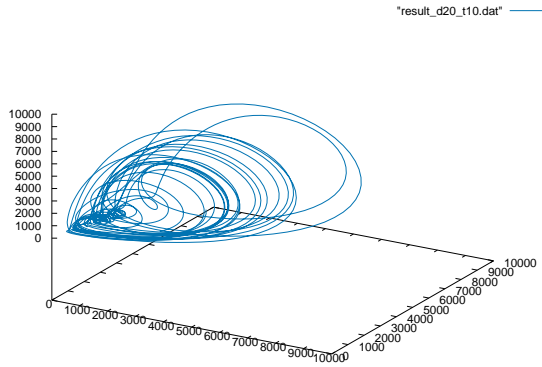
$$y(t) = \{x(t), x(t + \tau), \dots, x(t + (m - 1)\tau)\} \quad (1)$$

where  $x(t)$  means a scalar time series and  $\tau$  is the delay time.

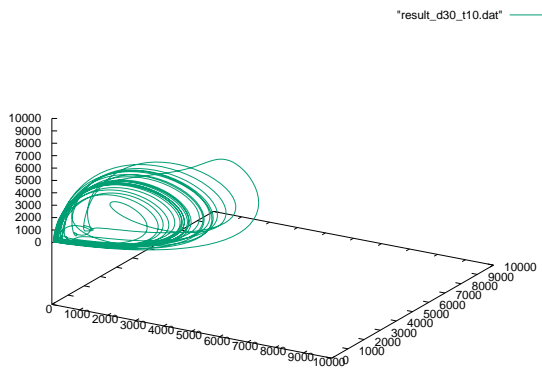
Figure 3 shows the simulation results when neuronal time-series data is embedded in 3-dimensional space with time delay  $\tau = 10$ . From this figure, we confirm that all three cultures exhibit a clear structure, because the orbit draws in certain range and does not move about randomly. Furthermore, in the case of the neurons at DIV 15 (Fig. 3(a)), the size of the attractor is larger and the behavior of the orbit is complex. As the culture matures, the attractor size becomes smaller and the complexity of the orbit becomes weaker.



(a) DIV 15.



(b) DIV 20.



(c) DIV 30.

Figure 3: Attractor reconstruction ( $\tau = 10$ ). x-axis:  $x(t)$ , y-axis:  $x(t + \tau)$ , z-axis:  $x(t + 2\tau)$ .

### 3.2 Recurrence plot

In 1987, Eckmann et al. introduced the method of recurrence plots (RPs) to visualize the recurrences of dynamical systems [7]. RPs shows when the time series visits the same region on the phase space. The recurrence of states in the phase space by a 2-dimensional plot is described by the following equation.

$$R(i, j) = \begin{cases} 1 & (\|\vec{x}(i) - \vec{x}(j)\| < \varepsilon) \\ 0 & (\text{otherwise}) \end{cases} \quad (2)$$

A recurrence is then defined when the distance between two states  $i$  and  $j$  (points on the trajectory) is smaller than a threshold  $\varepsilon$ . RP is a  $N \times N$  matrix of black and white dots in two time-axes. Using RPs for the analysis of time series, allows not only to visualize, but also to quantify the structures hidden in the data [8], [9].

The simulation results of RPs are shown in Fig. 4. The number of recurrence points increases with days. First two cases (Fig. 4(a) and (b)) show that the pattern of RPs has no regular form. In the last case (Fig. 4(c)), the pattern of RPs becomes more regular.

### 3.3 Lyapunov exponent

Lyapunov exponents provide a qualitative and quantitative characterization of the dynamical behavior. It is related to the exponentially fast divergence or convergence of nearby orbits in phase space. The Lyapunov exponent is used to determine whether a time series has a chaotic property in order to determine the sensitivity of the chaotic route to its initial conditions. The Lyapunov exponent is calculated by the following equation [10]. It is well known that the orbit is unstable and chaotic when  $\lambda$  has a positive value.

$$\lambda = \lim_{x \rightarrow \infty} \frac{1}{n} \sum_{i=1}^{n-1} \log \left| \frac{\Delta x_0}{\Delta x_n} \right| \quad (3)$$

The calculated Lyapunov exponents are summarized in Table 1. The Lyapunov exponents of all three networks have positive value. Namely, these neuronal time-series has chaotic property. The youngest culture (DIV 15) has the largest value of the Lyapunov exponent, and the value decreases as the culture matures.

Table 1: Lyapunov exponent.

neuron type	$\lambda$
DIV 15	3.82
DIV 20	3.20
DIV 30	2.54

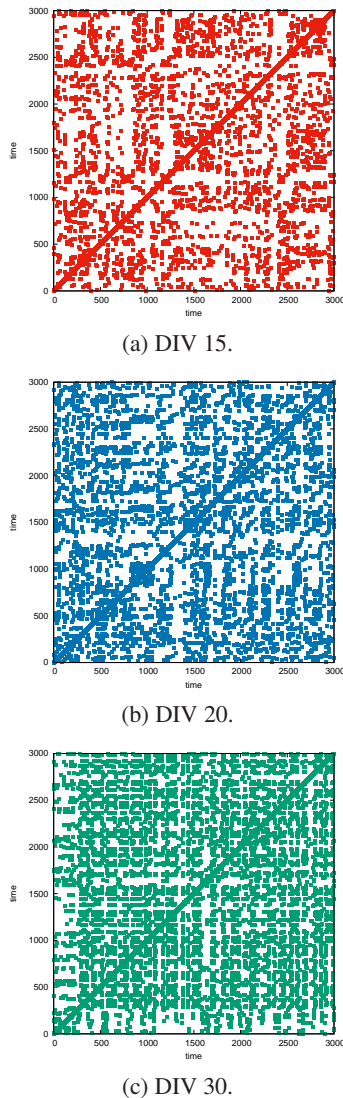


Figure 4: Recurrence plot ( $\varepsilon = 1.0$ ).

#### 4. Conclusions

In this study, we propose a visualization method for neuronal data using nonlinear time-series analysis. We used three recordings from neurons observed at different ages. By applying three nonlinear time-series analysis, we confirmed that the youngest neuron has the strongest activity and the neuronal behavior settles down as the culture matures.

In future works, we would like to calculate the characteristics of RPs, and to use data from different types of cells and conditions of the neuronal cultures. We are also interested to classify neuronal data using the techniques described here.

#### References

- [1] D. J. Bakkum, M. Radivojevic, U. Frey, F. Franke, A. Hierlemann and H. Takahashi, "Parameters for Burst Detection," *Frontiers in Computational Neuroscience*, doi: 10.3389/fncom.2013.00193, Jan. 2014.
- [2] E. Bradley and H. Kantz, "Nonlinear Time-Series Analysis Revisited," *Chaos*, vol. 25, doi: 10.1063/1.4917289, 2015.
- [3] M. E. J. Obien, K. Deligkaris, T. Bullmann, D. J. Bakkum, and U. Frey, "Revealing Neuronal Function through Microelectrode Array Recordings," *Frontiers in Neuroscience*, 8(423). <http://doi.org/10.3389/fnins.2014.00423>, 2015.
- [4] U. Frey, J. Sedivy, F. Heer, R. Pedron, M. Ballini, J. Mueller, A. Hierlemann, "Switch-Matrix-Based High-Density Microelectrode Array in CMOS Technology," *Solid-State Circuits, IEEE Journal Of*, 45(2), 467482. <http://doi.org/10.1109/JSSC.2009.2035196>, 2010.
- [5] D. J. Bakkum U. Frey, M. Radivojevic, T. L. Russell, J. Miller, M. Fiscella, A. Hierlemann, "Tracking Axonal Action Potential Propagation on a High-Density Microelectrode Array Across Hundreds of Sites," *Nature Communications*, 4, 2181. <http://doi.org/10.1038/ncomms3181>, 2013.
- [6] F. Takens, "Detecting Strange Attractors in Turbulence," In D.A. Rand and B.-S. Young, editors, *Dynamical Systems and Turbulence*, vol. 898 of Lecture Notes in Mathematics, pp. 366-381, Warwick 1980, 1981. Springer-Verlag, Berlin.
- [7] J. P. Eckmann, S. O. Kamphorst and D. Ruelle, "Recurrence Plots of Dynamical Systems," *Europhys. Lett.*, vol. 4, pp. 973, 1987.
- [8] M. Thiel, M. C. Romano and J. Kurths "How Much Information is Contained in a Recurrence Plot?," *Phys. Lett. A*, vol. 330, pp. 343-349, 2004.
- [9] N. Marwan, M. C. Romano, M. Thiel and J. Kurths, "Recurrence Plots for the Analysis of Complex Systems," *Physics Reports*, vol. 438, pp. 237-329, 2007.
- [10] A. Wolf, J. B. Swift, H. L. Swinney and J. A. Vastano, "Determining Lyapunov Exponents from a Time Series," *Physica D*, vol. 16, pp. 285-317, 1985.